



# Myocardial Coverage and Radiation Dose in Dynamic Myocardial Perfusion Imaging Using Third-Generation Dual-Source CT

Masafumi Takafuji, MD, Kakuya Kitagawa, MD, PhD, FSCCT, Masaki Ishida, MD, PhD, Yoshitaka Goto, MD, Satoshi Nakamura, MD, Naoki Nagasawa, RT, PhD, Hajime Sakuma, MD, PhD

All authors: Department of Radiology, Mie University Hospital, Mie, Japan

**Objective:** Third-generation dual-source computed tomography (3rd-DSCT) allows dynamic myocardial CT perfusion imaging (dynamic CTP) with a 10.5-cm z-axis coverage. Although the increased radiation exposure associated with the 50% wider scan range compared to second-generation DSCT (2nd-DSCT) may be suppressed by using a tube voltage of 70 kV, it remains unclear whether image quality and the ability to quantify myocardial blood flow (MBF) can be maintained under these conditions. This study aimed to compare the image quality, estimated MBF, and radiation dose of dynamic CTP between 2nd-DSCT and 3rd-DSCT and to evaluate whether a 10.5-cm coverage is suitable for dynamic CTP.

**Materials and Methods:** We retrospectively analyzed 107 patients who underwent dynamic CTP using 2nd-DSCT at 80 kV ( $n = 54$ ) or 3rd-DSCT at 70 kV ( $n = 53$ ). Image quality, estimated MBF, radiation dose, and coverage of left ventricular (LV) myocardium were compared.

**Results:** No significant differences were observed between 3rd-DSCT and 2nd-DSCT in contrast-to-noise ratio ( $37.4 \pm 11.4$  vs.  $35.5 \pm 11.2$ ,  $p = 0.396$ ). Effective radiation dose was lower with 3rd-DSCT ( $3.97 \pm 0.92$  mSv with a conversion factor of 0.017 mSv/mGy·cm) compared to 2nd-DSCT ( $5.49 \pm 1.36$  mSv,  $p < 0.001$ ). Incomplete coverage was more frequent with 2nd-DSCT than with 3rd-DSCT (1.9% [1/53] vs. 56% [30/54],  $p < 0.001$ ). In propensity score-matched cohorts, MBF was comparable between 3rd-DSCT and 2nd-DSCT in non-ischemic ( $146.2 \pm 26.5$  vs.  $157.5 \pm 34.9$  mL/min/100 g,  $p = 0.137$ ) as well as ischemic myocardium ( $92.7 \pm 21.1$  vs.  $90.9 \pm 29.7$  mL/min/100 g,  $p = 0.876$ ).

**Conclusion:** The radiation increase inherent to the widened z-axis coverage in 3rd-DSCT can be balanced by using a tube voltage of 70 kV without compromising image quality or MBF quantification. In dynamic CTP, a z-axis coverage of 10.5 cm is sufficient to achieve complete coverage of the LV myocardium in most patients.

**Keywords:** Multidetector computed tomography; Cardiac imaging techniques; Myocardial perfusion imaging; Image enhancement; Radiation dosage

## INTRODUCTION

During the last decade, CT has evolved from a morphologic modality for assessing coronary arteries to a functional modality for evaluating myocardial perfusion (1-3). There are currently two approaches in myocardial CT

perfusion imaging (CTP)—static and dynamic. Static CTP, which evaluates contrast distribution at a single time point, is easy to implement but limited in its ability to quantify myocardial blood flow (MBF) (4, 5). Dynamic CTP, on the other hand, allows full quantification of MBF and has shown promise in accurately detecting hemodynamically significant

Received May 7, 2019; accepted after revision August 30, 2019.

This study was partly supported by a departmental research grant from Siemens Japan.

**Corresponding author:** Kakuya Kitagawa, MD, PhD, FSCCT, Department of Radiology, Mie University Hospital, 2-174 Edobashi, Tsu, Mie 514-8507, Japan.

• Tel: (8159) 231-5029 • Fax: (8159) 232-8066 • E-mail: kakuya@clin.medic.mie-u.ac.jp

This is an Open Access article distributed under the terms of the Creative Commons Attribution Non-Commercial License (<https://creativecommons.org/licenses/by-nc/4.0>) which permits unrestricted non-commercial use, distribution, and reproduction in any medium, provided the original work is properly cited.

coronary artery stenosis (6-10). However, dynamic CTP techniques involve the acquisition of multiple consecutive phases and are therefore associated with higher radiation doses than are other CT scan techniques (11). Second-generation dual-source CT (2nd-DSCT) allows dynamic CTP to be performed at 80 kV with a mean effective dose of 6 mSv (12). However, coverage of the left ventricular (LV) myocardium is often incomplete under the available scan length of 7.3 cm (10).

Third-generation dual-source CT (3rd-DSCT) offers 10.5 cm of coverage, which is favorable in terms of myocardial coverage. However, it remains unclear whether 10.5 cm is sufficient to cover the entire LV myocardium. Moreover, the increased coverage results in increased radiation exposure if other conditions are kept the same. A previous phantom study of a simulated obese patient showed that 3rd-DSCT could perform coronary CT angiography (CCTA) at 70–80 kV without compromising image quality, as the system allowed a maximum tube current of 1300 mA at 70 kV (13). In comparison to the use of higher tube voltages, this approach can be expected to reduce the radiation dose in dynamic CTP at a maintained contrast-to-noise ratio (CNR) because iodinated contrast media show higher attenuation levels at lower X-ray tube voltages owing to a higher photoelectric effect and lesser Compton scattering (14-16).

The purpose of this study was to compare the image quality, estimated MBF, and radiation dose of dynamic CTP between 2nd-DSCT and 3rd-DSCT and to evaluate whether the 10.5-cm z-axis coverage was adequate for dynamic CTP.

## MATERIALS AND METHODS

### Subjects

This study was approved by the Institutional Review Board, and written informed consent for participation in the study was given by each patient. This was a retrospective analysis of a prospectively registered cohort at a single center. Using the cardiac CT registry at our institution (2, 6), we identified a total of 127 patients who had undergone stress dynamic CT using 2nd-DSCT (SOMATOM Definition Flash, Siemens Healthineers, Forchheim, Germany) or 3rd-DSCT (SOMATOM Force, Siemens Healthineers) between January and December 2015. The comprehensive CT protocol was indicated for patients who were referred for CCTA with known or suspected coronary artery disease. Patients with impaired renal function (estimated glomerular filtration rate < 30 mL/min/1.73 m<sup>2</sup> body surface area), known allergy to

iodinated contrast agent, or contraindications for adenosine were excluded from participation in the CT protocol.

Since the validity of MBF quantification in the presence of coronary artery bypass graft or persistent atrial fibrillation was unknown, patients with coronary arterial bypass graft (n = 15) and those with persistent atrial fibrillation (n = 5) were also excluded. Thus, the final study population consisted of 107 patients. Scans until June 2015 were performed with 2nd-DSCT at 80 kV (n = 54), and those since July 2015 have been performed with 3rd-DSCT at 70 kV (n = 53) (Fig. 1).

### CT Protocol

The CT protocol consisted of stress dynamic CTP, followed by CCTA and delayed enhancement CT. Dynamic CTP was performed with a bolus injection of 40 mL of iopamidol (flow rate, 5 mL/s) with an iodine concentration of 370 mgI/mL (Iopamiron 370; Bayer-Schering Pharma, Berlin, Germany) followed by 20 mL of saline (flow rate, 5 mL/s). After administering adenosine triphosphate (Adetphos-L, Kowa, Nagoya, Japan) at 0.16 mg/kg/min for 3 minutes, dynamic datasets were acquired for 30 seconds in the electrocardiographically triggered mode, with the table moving forward and backward between the two positions (i.e., “shuttle mode”) (10). The z-axis coverage of 2nd-DSCT and 3rd-DSCT was 73 mm and 105 mm, respectively. For heart rates ≤ 63 beats/min, the two table positions

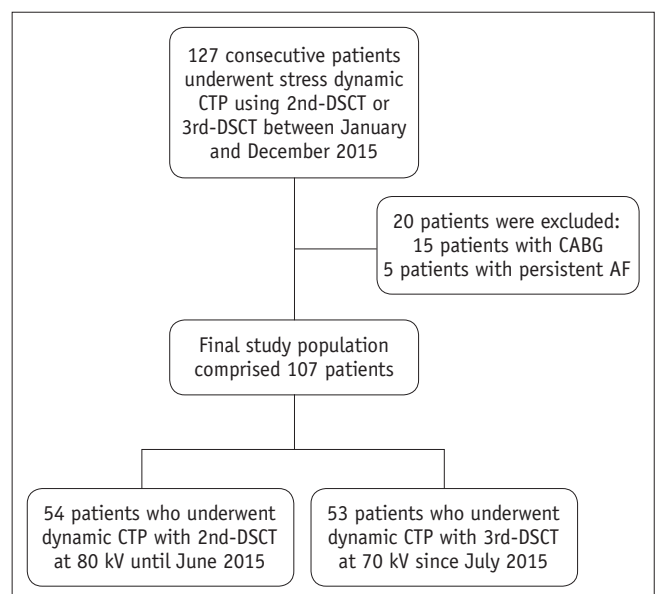


**Fig. 1. Flowchart shows patient selection protocol used to enroll patients in study.** AF = atrial fibrillation, CABG = coronary artery bypass graft, CTP = computed tomography perfusion imaging, 2nd-DSCT = second-generation dual-source computed tomography, 3rd-DSCT = third-generation dual-source computed tomography

were imaged in consecutive heartbeats. For heart rates > 63 beats/min, the other volume was covered every second heartbeat. Data were acquired at end-systole (250 ms after the R peak) with tube voltages of 80 kV and 70 kV with 2nd- and 3rd-DSCT, respectively. Tube current was determined using automatic tube current modulation (ATCM) with a quality reference of 350 mAs/rot at 120 kV for 2nd-DSCT and 300 mAs/rot at 80 kV for 3rd-DSCT, in accordance with the recommendations from the vendor.

Ten minutes after dynamic stress CTP, standard prospective CCTA covering the end-systole (250 ms after the R peak) to mid-diastole was performed at rest with the injection of 0.84 mL/kg of contrast medium over 12 seconds. Tube voltage was 2 x 100 kV or 80 kV in 2nd-DSCT and 2 x 80 kV or 70 kV, and tube current was determined using the automatic exposure control system with a quality reference of 300 mAs/rot at 120 kV in 3rd-DSCT and 350 mAs/rot at 120 kV in 2nd-DSCT. Gantry rotation time was 0.28 seconds in 2nd-DSCT and 0.25 seconds in 3rd-DSCT. Seven minutes after CCTA, end-systolic delayed-phase images were acquired without administration of any additional contrast medium by using electrocardiography-triggered axial scans at two alternating table positions (17, 18).

### CT Data Reconstruction and Image Post-Processing

All CCTA images were reconstructed with a medium soft convolution kernel (Bv40) by using iterative reconstruction (Advanced Modeled Iterative Reconstruction level 3). Dynamic CTP images and delayed-phase images were reconstructed in the axial plane with 3-mm slice thickness and 2-mm overlap with a medium sharp convolution kernel (Qr40 with 3rd-DSCT and B23 with 2nd-DSCT) without using iterative reconstruction because the iterative reconstruction technology is currently not compatible with the cardiac shuttle mode. The axial dynamic perfusion images were then processed using syngo.CT Myocardial Perfusion (Siemens Healthineers). As previously described (19), MBF was estimated using a dedicated parametric deconvolution technique based on a 2-compartment model of intra- and extravascular spaces to fit the time-attenuation curves using Volume Perfusion software (19). The algorithm then generated an MBF map with 3-mm thickness and 2-mm overlap by applying the maximum slope approach onto a model curve fit for every voxel.

### Image Analysis

To measure the degree of contrast enhancement and

image noise, a 5.0-cm<sup>2</sup> region of interest (ROI) was placed in the LV cavity on the axial dynamic CTP datasets with 5-mm slice thickness (11). Maximal enhancement was shown as the mean CT attenuation (in Hounsfield units [HU]) within the ROI at the time of peak LV enhancement. Image noise was measured as the standard deviation (SD) of CT attenuation within the ROI in the LV cavity on the first phase of dynamic CT images before the arrival of contrast medium. We also determined the CNR as follows (12):

$$\text{CNR} = (\text{HU}_{[\text{peak}]} - \text{HU}_{[\text{baseline}]}) / \text{noise}_{(\text{baseline})}$$

The MBF map (3-mm thickness) obtained using Volume Perfusion software was analyzed using in-house software written on Matlab (R2017a, Mathworks, Inc., Natick, MA, USA) to obtain mean MBF values in 16 segments (17 American Heart Association segments except for the apex). MBF in the non-ischemic myocardium was defined as the average MBF of the top three segments (12). Ischemic myocardium was defined as a segment with mean MBF value 75% or less of the highest MBF value within the 16 segments on the MBF map (2), and the minimal MBF of the ischemic segments was used to represent the MBF of ischemic myocardium of the patient.

The z-axis scan length required to cover the entire LV myocardium during end-systole was measured on CCTA using the multi-planar reconstruction function. Z-axis scan coverage actually obtained by stress CTP was measured on a time maximum intensity projection, which is a by-product of MBF quantification, by using Volume Perfusion software, reflecting the maximum value for the time phase direction from the dynamic volume data; next, the percentage of z-axis coverage by dynamic CTP was calculated (Fig. 2). When 50% or more of a segment was out of the scan range, the segment was counted as a missing segment and excluded from calculation of global MBF.

### Dose Estimation

Effective radiation doses were estimated by multiplying the dose-length product reported by the device by a conversion factor of 0.017 mSv/mGy·cm (20). The volumetric CT dose index (CTDIvol) was recorded for each study as reported by the scanner based on a 32-cm phantom.

### Statistical Analysis

Continuous variables are expressed as the mean and SD,

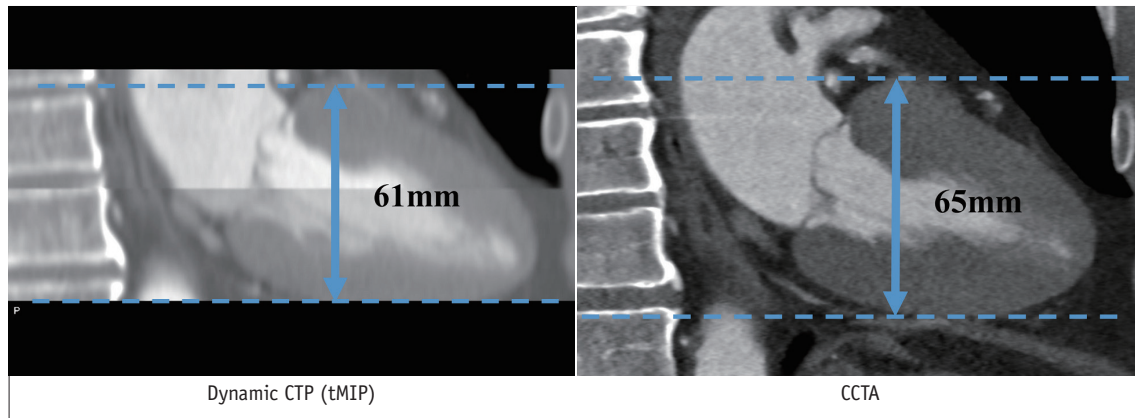


**Fig. 2.** Example of calculation for determining percentage z-axis coverage of LV myocardium on stress CTP. Z-axis coverage obtained by systolic stress CTP is 61 mm with 2nd-DSCT in this example, while 65 mm is required to cover entire LV myocardium according to systolic CCTA. Z-axis coverage in this case is therefore 94% (61 mm/65 mm). CCTA = coronary computed tomography angiography, LV = left ventricular, tMIP = time maximum intensity projection

while categorical variables are expressed as proportions. Student's *t* test was used to assess differences in continuous variables after examining the normality of the data. The chi-squared test was used to assess differences in proportion between categorical variables. Values of *p* < 0.05 were considered indicative of statistical significance. Absolute MBF values in 2nd-DSCT and 3rd-DSCT were compared in patients after propensity score matching. The propensity score was estimated from age, gender, hypertension, dyslipidemia, diabetes mellitus, smoking, body mass index (BMI), history of myocardial infarction, and percutaneous coronary intervention. We selected pairs of patients in the two groups (1:1 matching) using a nearest-neighbor matching algorithm within a caliper of 0.25 SD of the propensity score. This scoring and matching were performed after exclusion of patients with transmural infarction (*n* = 16) and those with non-ischemic cardiomyopathy (*n* = 4). Propensity score matching was performed using the SPSS statistical package (version 23.0, IBM Corp., Armonk, NY, USA). All the other statistical analyses were performed using JMP version 10 software (SAS Institute Inc., Cary, NC, USA).

## RESULTS

### Subject Characteristics

Subject characteristics are summarized in Table 1. No intergroup differences were observed with regard to gender, age, BMI, heart rate, risk factors, or medical history.

### Image Quality, MBF and Myocardial Coverage

Mean image noise in the left ventricle before the arrival

**Table 1.** Background Characteristics of Patients

Characteristics	3rd-DSCT at 70 kV (n = 53)	2nd-DSCT at 80 kV (n = 54)	<i>P</i>
Gender			
Male	30 (57)	40 (74)	0.058
Female	23 (43)	14 (26)	
Age (years)			
Mean ± SD	68.6 ± 10.0	69.2 ± 9.3	0.750
Range	36–84	41–87	
BMI (kg/m <sup>2</sup> )			
Mean ± SD	23.0 ± 2.7	23.2 ± 4.3	0.735
Range	14.8–30.4	16.0–40.6	
Heart rate (beats/min)			
Mean ± SD	75.9 ± 12.4	74.5 ± 11.3	0.541
Range	48–107	53–104	
Risk factor			
Hypertension	37 (70)	41 (76)	0.477
Hyperlipidemia	35 (66)	31 (57)	0.359
Diabetes	17 (32)	22 (41)	0.352
Smoking	27 (51)	31 (57)	0.502
History of CAD			
Known myocardial infarction	11 (21)	13 (24)	0.681
Prior PCI	23 (43)	18 (33)	0.284

Data are numbers of patients, with percentages in parentheses. BMI = body mass index, CAD = coronary artery disease, PCI = percutaneous coronary intervention, SD = standard deviation, 2nd-DSCT = second-generation dual-source computed tomography, 3rd-DSCT = third-generation dual-source computed tomography

of the contrast bolus was significantly higher with 3rd-DSCT at 70 kV (19.5 ± 2.8 HU) than with 2nd-DSCT at 80 kV (17.0 ± 2.8 HU, *p* < 0.001). However, no difference in CNR was seen between 3rd-DSCT at 70 kV (37.4 ± 11.4) and 2nd-

DSCT at 80 kV ( $35.5 \pm 11.2$ ,  $p = 0.396$ ) due to the higher maximal enhancement with 3rd-DSCT at 70 kV ( $757.6 \pm 156.5$  HU) compared to that with 2nd-DSCT at 80 kV ( $632.7 \pm 141.2$  HU,  $p < 0.001$ ) (Fig. 3A).

Propensity score matching yielded a total of 34 matched pairs. In these matched cohorts, there was no significant difference in any clinical factors between 3rd-DSCT and 2nd-DSCT (Table 2). Among the matched pairs, 11 patients who underwent 3rd-DSCT and 12 patients who underwent 2nd-DSCT had ischemic segments ( $p = 0.798$ ). There was no significant difference between 3rd-DSCT and 2nd-DSCT in the MBF of non-ischemic ( $146.2 \pm 26.5$  vs.  $157.5 \pm 34.9$  mL/min/100 g,  $p = 0.137$ ) and ischemic myocardium ( $92.7 \pm 21.1$  vs.  $90.9 \pm 29.7$  mL/min/100 g,  $p = 0.876$ ).

The z-axis coverage required to cover the LV myocardium measured on end-systolic CCTA was  $61.6 \pm 7.1$  mm (range: 48–81 mm) and  $62.9 \pm 7.2$  mm (range: 48–76 mm) in patients scanned using 3rd-DSCT and 2nd-DSCT, respectively ( $p = 0.349$ ), while the z-axis length of the LV myocardium actually covered by stress dynamic CTP was  $61.4 \pm 7.1$  mm and  $59.7 \pm 4.6$  mm, respectively ( $p = 0.150$ ). Percentage z-axis coverage of the LV myocardium was significantly higher with 3rd-DSCT ( $99.7 \pm 2.0\%$ ) than with 2nd-DSCT ( $95.5 \pm 5.5\%$ ,  $p < 0.001$ ). Perfusion scans in 8 consecutive

patients using 2nd-DSCT and 3rd-DSCT are presented in Figure 4 for comparisons of the z-axis coverage.

The z-axis coverage of stress CTP using 2nd-DSCT was incomplete ( $< 100\%$ ) in 56% of the patients (30 of 54), with partial coverage of either the anterior wall ( $n = 9$ ),

**Table 2. Clinical Factors of Propensity Score-Matched Patients**

Characteristics	3rd-DSCT at 70 kV (n = 34)	2nd-DSCT at 80 kV (n = 34)	P
<b>Gender</b>			
Male	20 (59)	21 (62)	0.804
Female	14 (41)	13 (38)	
<b>Age (years)</b>			
Mean $\pm$ SD	$68.5 \pm 9.6$	$67.5 \pm 9.7$	0.652
<b>BMI (kg/m<sup>2</sup>)</b>			
Mean $\pm$ SD	$23.3 \pm 2.4$	$23.2 \pm 4.9$	0.971
<b>Risk factor</b>			
Hypertension	25 (74)	24 (71)	0.787
Hyperlipidemia	21 (62)	20 (59)	0.804
Diabetes	11 (32)	10 (29)	0.793
Smoking	15 (44)	17 (50)	0.627
<b>History of CAD</b>			
Known myocardial infarction	3 (9)	4 (12)	0.690
Prior PCI	10 (29)	11 (32)	0.793

Data are numbers of patients, with percentages in parentheses.

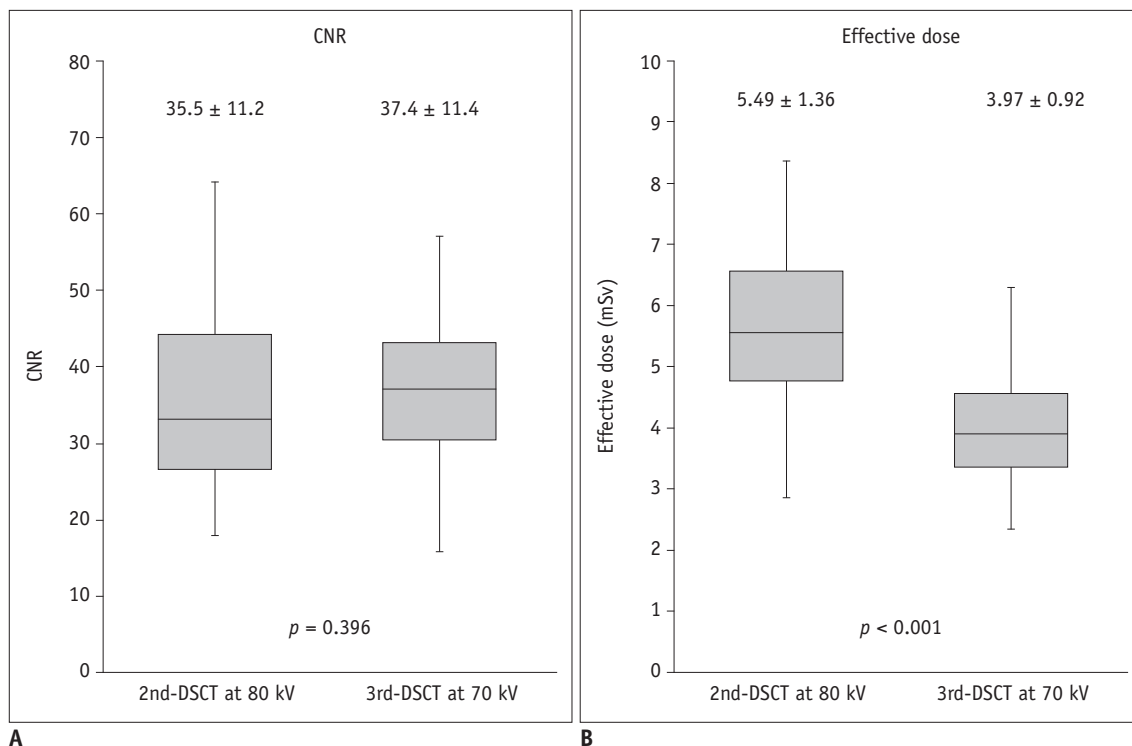


**Fig. 3. Box plots of CNR (A) and effective dose (B) of 2nd-DSCT at 80 kV and 3rd-DSCT at 70 kV.** Center lines show medians, box limits indicate 25th and 75th percentiles, and whiskers extend 1.5-times interquartile range from 25th to 75th percentiles. CNR = contrast-to-noise ratio



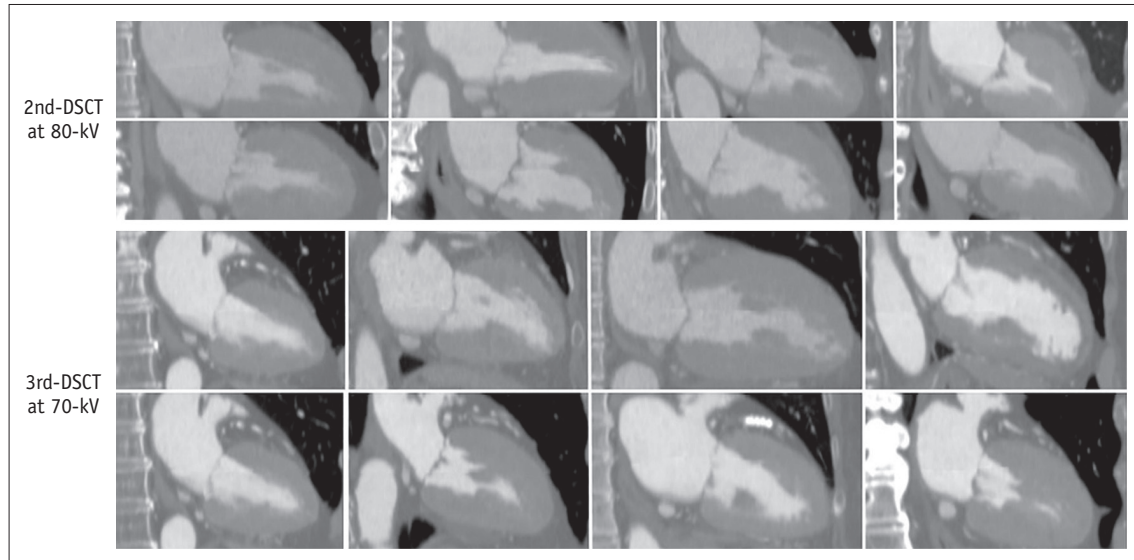


**Fig. 4.** tMIP of stress dynamic CTP with 2nd-DSCT at 80 kV and 3rd-DSCT at 70 kV in 8 consecutive patients, respectively. Z-axis coverage of 2nd-DSCT is incomplete in all of presented cases. On the other hand, entire LV myocardium is covered in all cases with 3rd-DSCT.

inferior wall ( $n = 10$ ), or both ( $n = 11$ ), while incomplete coverage was seen with 3rd-DSCT in only 1 patient (1/53, 1.9%,  $p < 0.001$ ), involving partial coverage of the anterior wall due to difficulty in breath-holding. The number of missing segments (50% or more of the segment is outside the z-axis scan length) was 35 in 21 patients (4%, 35/864) scanned with 2nd-DSCT and 2 in 1 patient (0.2%, 2/848,  $p < 0.001$ ) scanned with 3rd-DSCT. The number of missing segments per patient in 2nd-DSCT was 3 in 4 patients, 2 in 6 patients, and 1 in 11 patients. Representative dynamic CTP images with 2nd-DSCT and 3rd-DSCT are presented in Figures 5 and 6, respectively.

#### Radiation Dose

The number of dynamic phases did not differ significantly between 3rd-DSCT ( $11.5 \pm 1.4$ ) and 2nd-DSCT ( $12.0 \pm 1.5$ ,  $p = 0.116$ ). Mean radiation dose per phase was significantly reduced with 3rd-DSCT at 70 kV ( $0.35 \pm 0.07$  mSv) in comparison with that at 2nd-DSCT at 80 kV ( $0.46 \pm 0.10$  mSv,  $p < 0.001$ ). Similar results were observed for the effective dose of the entire CTP (mean,  $3.97 \pm 0.92$  vs.  $5.49 \pm 1.36$  mSv, respectively;  $p < 0.001$ ) (Fig. 3B). On average, the effective radiation dose with 3rd-DSCT was 27.6% lower than that with 2nd-DSCT. Mean CTDI<sub>vol</sub> was  $22.3 \pm 5.3$  mGy and  $45.5 \pm 10.3$  mGy, respectively, for patients imaged with 3rd-DSCT at 70 kV and 2nd-DSCT at 80 kV ( $p < 0.001$ ). Mean tube currents using 3rd-DSCT ( $642 \pm 139$  mA) and 2nd-DSCT ( $645 \pm 129$  mA) did not differ significantly ( $p = 0.908$ ). Maximum tube current was 976 mA and 771 mA for 3rd-

DSCT and 2nd-DSCT, respectively. The results are summarized in Table 3. The total radiation dose of CT examination, including CCTA and delayed enhancement, was  $8.66 \pm 2.52$  mSv and  $11.65 \pm 2.29$  mSv for 3rd-DSCT and 2nd-DSCT, respectively.

#### DISCUSSION

This study demonstrated that: 1) the z-axis coverage of 10.5 cm in 3rd-DSCT was sufficient to evaluate perfusion of the entire LV myocardium by dynamic myocardial CTP, while myocardial coverage was incomplete in 56% of patients with the coverage available in 2nd-DSCT (7.3 cm); and 2) dynamic CTP at 70 kV using 3rd-DSCT allows for a nearly 30% reduction in radiation dose despite the 50% widening of the z-axis coverage in comparison to CTP at 80 kV using 2nd-DSCT, without compromising image quality.

Dynamic CTP allows noninvasive quantification of MBF from the time-attenuation curves of both the blood pool and the myocardium, independent of the optimal selection of the data acquisition time point, and may thus allow more precise identification of the hemodynamic relevance of luminal stenosis in comparison with static CTP (10). One of the limitations of dynamic CTP has been the limited scan length along the z-axis, which may result in incomplete coverage of the LV myocardium. This study systematically evaluated whether the z-axis coverage of LV myocardium of 2nd-DSCT (7.3 cm) or 3rd-DSCT (10.5 cm) was sufficient for whole-heart dynamic CTP. A previous study reported

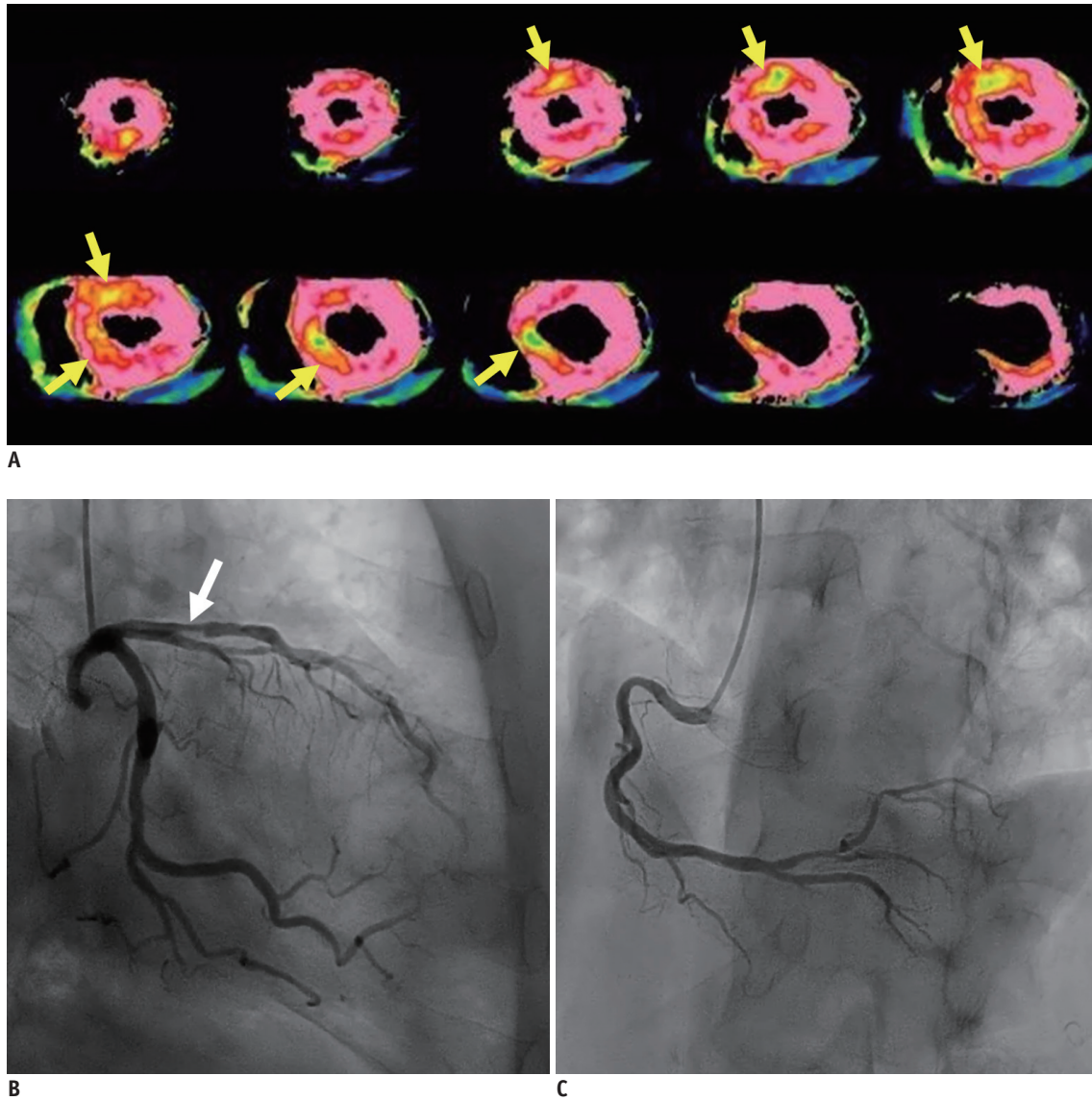


**Fig. 5. Dynamic CTP using 2nd-DSCT in 71-year-old man.**

Short-axis MBF maps (A) show mildly reduced perfusion in anteroseptal wall (arrows). Coronary angiography demonstrated moderate stenosis in left anterior descending artery (arrow) (B), while no stenosis was found in right coronary artery (C). Although z-axis scan length of 7.3 cm resulted in incomplete (96%) myocardial coverage with partial missing of basal anterior wall in this patient, all myocardial segments were still assessable. MBF = myocardial blood flow

that approximately one-third of CTP procedures performed using 2nd-DSCT resulted in incomplete coverage under the available scan length of 7.3 cm (10). We found that incomplete coverage was more frequent (involving > 50% of examinations) in 2nd-DSCT, although the risk of missing 3 segments was still low (4/54, 7.4%). With 3rd-DSCT, myocardial coverage was almost always complete, with only 1 case missing 2 segments due to difficulty in breath-holding. Although wide-detector CT with scan lengths up to 16 cm offers clear advantages in z-axis coverage (21), 10.5 cm seems sufficient to cover the entire LV myocardium

in most patients, as demonstrated from the current results, and may be good enough to cover the entire coronary artery tree, potentially eliminating the need for separate acquisition of CCTA (22).

For dose reduction of dynamic CTP in this study, we used a combination of low tube voltage and ATCM. Lowering tube potential is a well-recognized strategy to reduce radiation, because radiation doses vary approximately with the square of tube voltage. Diagnostic image quality can be maintained despite the higher image noise at lower tube potentials due to the higher attenuation of iodine at low photon energies,

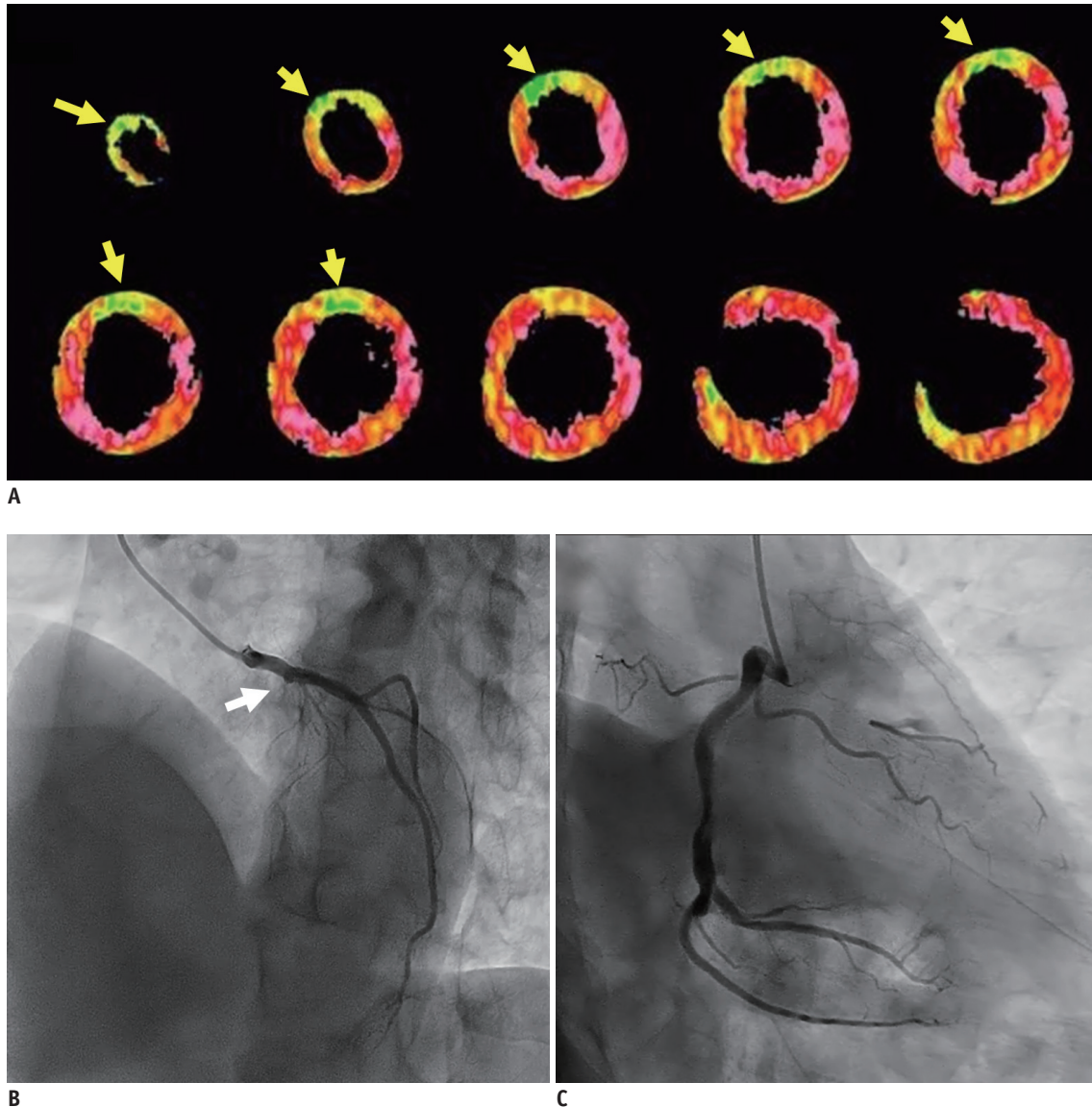


**Fig. 6. Dynamic CTP using 3rd-DSCCT in 55-year-old man.**

Short-axis MBF maps (A) show severely reduced perfusion in anteroseptal wall (arrows). Coronary angiography demonstrated total occlusion in proximal left anterior descending artery (arrow) (B) with collateral vessel from right coronary artery (C). Dynamic CTP with z-axis scan length of 10.5 cm provided complete coverage of LV myocardium.

thus increasing intravascular contrast (13). Fujita et al. (12) demonstrated that dynamic CTP imaging using 2nd-DSCCT with 80 kV/370 mAs instead of 100 kV/300 mAs was associated with a 40% reduction in mean radiation dose. ATCM allows maintenance of constant image quality with reduced radiation exposure by estimating optimal tube current values from topogram data. Moreover, the tube current is fine-tuned according to the actual attenuation measured 180° earlier in the tube rotation, adjusting to the dynamic change of attenuation characteristics over time during the first-pass of contrast medium through the heart (23). Kim et al. (11) found that the use of ATCM resulted

in a reduction in the mean effective radiation dose in comparison with a fixed tube current, while still providing diagnostically acceptable images.

In the current study, an even lower tube voltage (70 kV) was used together with ATCM to avoid the radiation increase inherent in wider coverage, successfully reducing radiation exposure by 30% compared to 80 kV with ATCM ( $3.97 \pm 0.92$  mSv vs.  $5.49 \pm 1.36$  mSv, respectively). Although the image noise was always higher at 70 kV, as expected, CNR was maintained due to the higher contrast enhancement.

Some limitations must be considered when interpreting the results from the present study. First, BMI in most of



**Table 3. Summary of Study Results**

	3rd-DSCT 70-kV/AEC (n = 53)	2nd-DSCT 80-kV/AEC (n = 54)	P
Percentage z-axis coverage of myocardium (%)	99.7 ± 2.0	95.5 ± 5.5	< 0.001
Image noise (HU)	19.5 ± 2.8	17.0 ± 2.8	< 0.001
Maximal enhancement (HU)	757.6 ± 156.5	632.7 ± 141.2	< 0.001
CNR	37.4 ± 11.4	35.5 ± 11.2	0.396
Effective dose per phase (mSv)	0.35 ± 0.07	0.46 ± 0.10	< 0.001
Number of dynamic phases	11.5 ± 1.5	12.0 ± 1.5	0.116
Effective dose (mSv)	3.97 ± 0.92	5.49 ± 1.36	< 0.001
CTDIvol (mGy)	22.3 ± 5.3	45.5 ± 10.3	< 0.001
Tube current (mA)	642 ± 139	645 ± 129	0.908

AEC = automatic exposure control, CNR = contrast-to-noise ratio, CTDIvol = volumetric CT dose index, HU = Hounsfield units

the patient population was < 25 kg/m<sup>2</sup>. The applicability of 70 kV for overweight or obese patients remains unclear. However, the X-ray tube for 3rd-DSCT systems allows dynamic CTP with a maximum tube current of 1300 mA at a low-kV range (70, 80, or 90 kV) (13, 14), much higher than the maximum tube current actually emitted for dynamic CTP in 3rd-DSCT (976 mA) in our study population. Second, MBF values were not validated against a gold standard such <sup>15</sup>O-H<sub>2</sub>O positron emission tomography in our study. A linear correlation between CT-derived MBF measurements and microsphere-derived MBF has been demonstrated in a porcine animal model at 100 kV (24). Theoretically, the use of 70 kV or 80 kV instead of 100 kV would not affect the quantification obtained with this technique, since the linear relationship between contrast concentration and attenuation would not be compromised with a lower tube voltage. Nonetheless, the similar estimated MBF values between 70 kV and 80 kV after propensity score matching in our study do not guarantee a homogenous quantification performance because MBF quantification can be largely affected by the physiologic response to adenosine. Lastly, we did not evaluate the incidence of artifacts such as beam-hardening, scatter, and motion on dynamic CTP with 2nd- and 3rd-DSCT.

In conclusion, the z-axis coverage of 10.5 cm in dynamic CTP was sufficient to cover the entire LV myocardium in most patients. Despite this increased coverage, dynamic CTP was successfully performed with a mean effective dose of only 3.97 mSv without compromising image quality or MBF quantification.

#### Conflicts of Interest

One of the authors (H.S.) received a research grant from

DAIICHI SANKYO COMPANY, LIMITED, Fuji Pharma Co., Ltd., FUJIFILM RI Pharma Co., Ltd., Eisai Co., Ltd. All the authors have nothing to disclose.

#### ORCID iDs

Kakuya Kitagawa

<https://orcid.org/0000-0003-4402-6846>

Masafumi Takafuji

<https://orcid.org/0000-0002-6883-8059>

Masaki Ishida

<https://orcid.org/0000-0003-0625-0767>

Yoshitaka Goto

<https://orcid.org/0000-0002-8342-5578>

Satoshi Nakamura

<https://orcid.org/0000-0002-9634-9332>

Naoki Nagasawa

<https://orcid.org/0000-0002-0393-5421>

Hajime Sakuma

<https://orcid.org/0000-0003-3547-2940>

#### REFERENCES

- Schuijf JD, Ko BS, Di Carli MF, Hislop-Jambrich J, Ithdayhid AR, Seneviratne SK, et al. Fractional flow reserve and myocardial perfusion by computed tomography: a guide to clinical application. *Eur Heart J Cardiovasc Imaging* 2018;19:127-135
- Nakamura S, Kitagawa K, Goto Y, Omori T, Kurita T, Yamada A, et al. Incremental prognostic value of myocardial blood flow quantified with stress dynamic computed tomography perfusion imaging. *JACC Cardiovasc Imaging* 2019;12(7 Pt 2):1379-1387
- Kitagawa K, Goto Y, Nakamura S, Takafuji M, Hamdy A, Ishida M, et al. Dynamic CT perfusion imaging: state of the art. *Cardiovasc Imaging Asia* 2018;2:38-48

4. Yang DH, Kim YH, Roh JH, Kang JW, Han D, Jung J, et al. Stress myocardial perfusion CT in patients suspected of having coronary artery disease: visual and quantitative analysis-validation by using fractional flow reserve. *Radiology* 2015;276:715-723
5. Rochitte CE, George RT, Chen MY, Arbab-Zadeh A, Dewey M, Miller JM, et al. Computed tomography angiography and perfusion to assess coronary artery stenosis causing perfusion defects by single photon emission computed tomography: the CORE320 study. *Eur Heart J* 2014;35:1120-1130
6. Goto Y, Kitagawa K, Uno M, Nakamori S, Ito T, Nagasawa N, et al. Diagnostic accuracy of endocardial-to-epicardial myocardial blood flow ratio for the detection of significant coronary artery disease with dynamic myocardial perfusion dual-source computed tomography. *Circ J* 2017;81:1477-1483
7. Coenen A, Lubbers MM, Kurata A, Kono A, Dedic A, Chelu RG, et al. Diagnostic value of transmural perfusion ratio derived from dynamic CT-based myocardial perfusion imaging for the detection of haemodynamically relevant coronary artery stenosis. *Eur Radiol* 2017;27:2309-2316
8. Vliegenthart R, De Cecco CN, Wichmann JL, Meinel FG, Pelgrim GJ, Tesche C, et al. Dynamic CT myocardial perfusion imaging identifies early perfusion abnormalities in diabetes and hypertension: insights from a multicenter registry. *J Cardiovasc Comput Tomogr* 2016;10:301-308
9. Rossi A, Dharampala A, Wragg A, Davies LC, van Geuns RJ, Anagnostopoulos C, et al. Diagnostic performance of hyperaemic myocardial blood flow index obtained by dynamic computed tomography: does it predict functionally significant coronary lesions? *Eur Heart J Cardiovasc Imaging* 2014;15:85-94
10. Bamberg F, Becker A, Schwarz F, Marcus RP, Greif M, von Ziegler F, et al. Detection of hemodynamically significant coronary artery stenosis: incremental diagnostic value of dynamic CT-based myocardial perfusion imaging. *Radiology* 2011;260:689-698
11. Kim SM, Kim YN, Choe YH. Adenosine-stress dynamic myocardial perfusion imaging using 128-slice dual-source CT: optimization of the CT protocol to reduce the radiation dose. *Int J Cardiovasc Imaging* 2013;29:875-884
12. Fujita M, Kitagawa K, Ito T, Shiraishi Y, Kurobe Y, Nagata M, et al. Dose reduction in dynamic CT stress myocardial perfusion imaging: comparison of 80-kV/370-mAs and 100-kV/300-mAs protocols. *Eur Radiol* 2014;24:748-755
13. Meinel FG, Canstein C, Schoepf UJ, Sedlmaier M, Schmidt B, Harris BS, et al. Image quality and radiation dose of low tube voltage 3rd generation dual-source coronary CT angiography in obese patients: a phantom study. *Eur Radiol* 2014;24:1643-1650
14. Meyer M, Haubenreisser H, Schoepf UJ, Vliegenthart R, Leidecker C, Allmendinger T, et al. Closing in on the K edge: coronary CT angiography at 100, 80, and 70 kV-initial comparison of a second- versus a third-generation dual-source CT system. *Radiology* 2014;273:373-382
15. Nakayama Y, Awai K, Funama Y, Hatemura M, Imuta M, Nakaura T, et al. Abdominal CT with low tube voltage: preliminary observations about radiation dose, contrast enhancement, image quality, and noise. *Radiology* 2005;237:945-951
16. Bahner ML, Bengel A, Brix G, Zuna I, Kauczor HU, Delorme S. Improved vascular opacification in cerebral computed tomography angiography with 80 kVp. *Invest Radiol* 2005;40:229-234
17. Kurobe Y, Kitagawa K, Ito T, Kurita Y, Shiraishi Y, Nakamori S, et al. Myocardial delayed enhancement with dual-source CT: advantages of targeted spatial frequency filtration and image averaging over half-scan reconstruction. *J Cardiovasc Comput Tomogr* 2014;8:289-298
18. Kurita Y, Kitagawa K, Kurobe Y, Nakamori S, Nakajima H, Dohi K, et al. Estimation of myocardial extracellular volume fraction with cardiac CT in subjects without clinical coronary artery disease: a feasibility study. *J Cardiovasc Comput Tomogr* 2016;10:237-241
19. Mahnken AH, Klotz E, Pietsch H, Schmidt B, Allmendinger T, Haberland U, et al. Quantitative whole heart stress perfusion CT imaging as noninvasive assessment of hemodynamics in coronary artery stenosis: preliminary animal experience. *Invest Radiol* 2010;45:298-305
20. Einstein AJ, Moser KW, Thompson RC, Cerqueira MD, Henzlova MJ. Radiation dose to patients from cardiac diagnostic imaging. *Circulation* 2007;116:1290-1305
21. So A, Imai Y, Nett B, Jackson J, Nett L, Hsieh J, et al. Technical note: evaluation of a 160-mm/256-row CT scanner for whole-heart quantitative myocardial perfusion imaging. *Med Phys* 2016;43:4821
22. Yi Y, Wu W, Lin L, Zhang HZ, Qian H, Shen ZJ, et al. Single-phase coronary artery CT angiography extracted from stress dynamic myocardial CT perfusion on third-generation dual-source CT: validation by coronary angiography. *Int J Cardiol* 2018;269:343-349
23. Kalra MK, Maher MM, Toth TL, Schmidt B, Westerman BL, Morgan HT, et al. Techniques and applications of automatic tube current modulation for CT. *Radiology* 2004;233:649-657
24. Bamberg F, Hinkel R, Schwarz F, Sandner TA, Baloch E, Marcus R, et al. Accuracy of dynamic computed tomography adenosine stress myocardial perfusion imaging in estimating myocardial blood flow at various degrees of coronary artery stenosis using a porcine animal model. *Invest Radiol* 2012;47:71-77